Contents lists available at ScienceDirect

Chemical Engineering Research and Design

journal homepage: www.elsevier.com/locate/cherd

Impact of solid and gas flow patterns on solid mixing in bubbling fluidized beds

Yunning Li[a,c], *Jingguo Rong*[b], *Kai Zhang*[b], *Xiangfeng Fan*[c,*]

[a] *China Electricity Council, Beijing, 100761, China*
[b] *North China Electric Power University, Beijing, 102206, China*
[c] *Institute for Materials and Processes, School of Engineering, The University of Edinburgh, Edinburgh EH9 3JL, UK*

ARTICLE INFO

Article history:
Received 31 July 2017
Received in revised form 29 November 2017
Accepted 8 December 2017
Available online xxx

Keywords:
Bubbling fluidization
Flow structure
Mixing
Active index
Flow pattern

ABSTRACT

Bubbling fluidization has been widely applied in industrial processes as an effective means for providing excellent mixing, good heat and mass transfer. Examples include granulation, coating, mixing, power generation from coal, renewable energy production, gasification and pyrolysis. In this study, we attempted to analyse the impact of solid flow patterns, bed design and operational conditions on solid mixing in a bubbling fluidized bed. The solid mixing behaviour was estimated based on the dispersion coefficient of particles, the active index (AI), and the distribution of particle residence time within the entire bed. In our previous studies, four flow patterns have been founded and classified as patterns A, B, C and D. Results presented from this study indicate that the mixing behaviour in a fluidized bed varies significantly with solid flow patterns which is a result of a combination of operational conditions, properties of bed materials and bed designs. Flow pattern D provides the best mixing in the four flow patterns identified by using the PEPT technique. Pattern A provides the worst solid mixing. Pattern B is a typical solid flow pattern reported in literature, but its mixing behaviour is only better than the Pattern A.

1. Introduction

Bubbling fluidization has been employed to many industrial processes, such as granulation, coating and drying, mixing, coal combustion and gasification, renewable energy production, chemical, petrochemical and metallurgical processes (Maio et al., 2013; Sette et al., 2015a, 2015b). It has been demonstrated that the granulation and mixing efficiency, heat and mass transfer, and energy consumption (He et al. 2004; Shibata et al. 1991) depend on solid/gas flow structure or solid/gas flow pattern. Intensive research has been conducted to investigate the fluidization behaviour experimentally and numerically (Herzog et al. 2012; Salman and Hounslow, 2007), and many models have been developed for identifying the effect of operational conditions, particle properties and bed design on fluidization behaviour and mixing, and for optimizing reactor design and bed scale up. For example, Olsson et al. (2012) experimentally investigated the fuel dispersion in a large scale bubbling fluidized bed with a cross section area of 1.44 m^2 through analysing the effect of operational conditions and fuel particle properties on the local mixing mechanisms and lateral fuel dispersion. Li et al. (2014) proposed an energy minimization multi-scale model (EMMS) to characterize the meso-scale structure of fluidization. Ku et al. (2013) used an Eulerian–Lagrangian approach to simulate a bubbling fluidized bed and analysed solid flow pattern, bed expansion, pressure drop and fluctuation by considering drag force correlations, particle–particle and particle-wall collisions. Wang et al. (2014) developed a drag model to simulate the meso-scale structure in solid-gas bubbling fluidized beds.

However many factors can affect solid/gas flow pattern and solid mixing in a fluidized bed and make fundamental analysis, modelling and prediction of fluidization behaviour difficult and in some cases impossible (Garcia-Gutierrez et al., 2013; Laverman et al. 2012). All of these factors are interrelated, and their relative importance is unclear. Various techniques have been proposed to experimentally estimate the solid mixing in fluidized beds since the late 1940s (Gorji-Kandi et al., 2015; Kunii and Levenspiel, 1991; Sánchez-Prieto et al., 2017; Sette et al., 2015a; Xiao et al., 1998). For example, Lim et al. (1993) and Grasa and Abanades (2002) used a layer of tracer particles placed

* *Corresponding author.*
E-mail address: x.fan@ed.ac.uk (X. Fan).

https://doi.org/10.1016/j.cherd.2017.12.014

horizontally inside fluidized beds and measured the tracer concentration in collected samples. Bokkers et al. (2004), Lam Cheun U (2010), Gorji-Kandi et al. (2015), and Sánchez-Prieto et al. (2017) placed two types of particles at different levels of the bed to examine the extent of their intermixing (Kunii and Levenspiel, 1991). Avidan and Yerushalmi (1985), Du et al. (2002), Bellgardt and Werther (1986), and Chirone et al. (2004) introduced tracer particles by step- or pulse-injection into the bed to determine the residence time distribution and concentration of the tracer particles (Kunii and Levenspiel, 1991). Pallares and Johnsson (2006) followed individual tracer particles in a 2-D fluidized bed for a long period of time to examine the solid mixing profile (Kunii and Levenspiel, 1991; Lam Cheun U, 2010). Despite this wealth of different approaches, experimental difficulties have always arisen due to the highly dynamic and complicated flow structure within the fluidized bed (Bi et al., 2000; Fan et al., 2011; Pallares and Johnsson, 2006) and the lack of an appropriate measurement technique (Avidan and Yerushalmi, 1985; Grasa and Abanades, 2002; Lam Cheun U, 2010). For example, most of the aforementioned techniques are invasive and affect the solid flow structure within the bed, therefore the results may not reflect the actual mixing under the operational conditions. In the cases where tracer particles are arranged within the bed before the bed has been fluidized, a regime transition from the static bed to fluidized bed takes place. The transition can alter the tracer concentration before the bed reaches the steady fluidization state. The injection of tracer particles into the fluidized bed can also disturb the local flow structure and subsequently influence the results (Lam Cheun U, 2010). In our previous studies, PEPT was used to map the solid and gas flow patterns, the impact of particle size, particle density, bed design and operational conditions on solid and gas flow patterns. Four solid flow patterns have been founded under various fluidization conditions, and a method for the prediction of solid flow patterns based on operational condition and particle properties has also be reported in our previous study (Fan et al., 2008a, 2008b, 2011; Li et al. 2014). Solid mixing behaviour in a fluidized bed is usually evaluated in terms of solid dispersion coefficient and mixing indexes. However, the results vary significantly with the techniques and models used (Avidan and Yerushalmi, 1985; Kunii and Levenspiel, 1991; Mostoufi and Chaouki, 2001; Sánchez-Prieto et al., 2017; Sette et al., 2016; Sette et al., 2015b; Shao et al., 2016; Stein, 1999; Zhang et al., 2009). For example, the dispersion coefficient is usually obtained by fitting one of the two most popular models to the experimental data (Dennis, 2013; Kunii and Levenspiel, 1991; Lam Cheun U, 2010; Liu and Chen, 2010; Sánchez-Prieto et al., 2017), these models have their restrictions and limitations (Avidan and Yerushalmi, 1985; Lam Cheun U, 2010; Shen and Zhang, 1998).

In this study, we use PEPT to directly measure the solid flow patterns and investigate the effect of solid flow patterns and operational conditions on solid mixing. The dispersion coefficients, the distribution of average residence time of the particle at different regions of the bed of particles were calculated based on particle trajectories. An active index (AI) has been developed to evaluate the solid mixing by understanding the frequency and opportunity of particles travelling to different regions within the fluidized beds. The dispersion coefficient was calculated based on the method proposed by Stein (1999) and Parker et al. (1997).

2. Materials and methods

The experiment setup consisted of a fluidized bed and a PEPT tracking system, as shown in Fig. 1. The fluidized bed was a Plexiglas-made cylindrical column with 0.152 m I.D. and 1.000 m height. Two types of air distributors used in this study were sintered metal filter plates with average pore diameters of 1 μm, 10 μm and 15 μm, and stainless steel wire meshes with pore diameters of 60 μm and 230 μm. Air under ambient conditions was supplied by a GA11CFF compressor and injected into the bed through a cone section. The air flowrate was measured and controlled with calibrated rota-meters. The bed pressure was measured with a FC0510 micro-manometer interfaced to a PC through a RS232 port. Glass beads and silica sand as shown in Table 1 were used as the bed materials. They belong to group B particles according to the Geldart classification (Geldart, 1973).

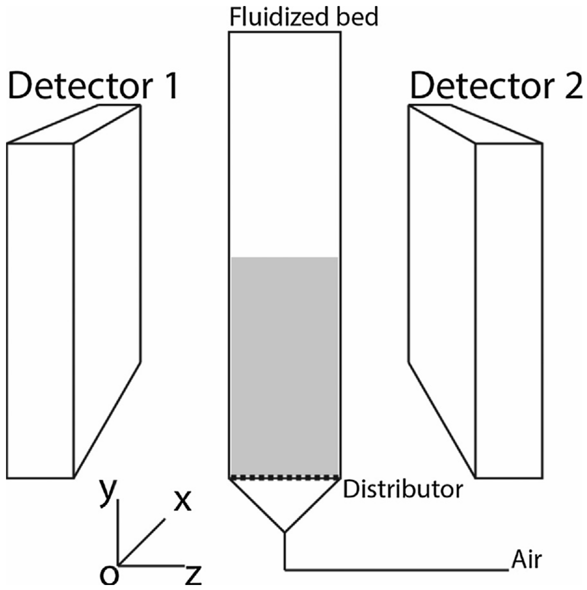

Fig. 1 – Schematic diagram of experimental setup.

Table 1 – Properties of bed materials.

Bed material	Silica sand	Glass bead
Particle density (kg/m^3)	2700	2700
Particle size (mm)	60–210	220–470
Mean size (mm)	117	352
u_{mf} (m/s)	0.046	0.15
Pore size of the air distributor (mm)	1	1, 10, 15, 60, 230
H/D	1, 1.5, 2	1, 1.5, 2
Superficial gas velocity (m/s)	0.17, 0.22, 0.34, 0.40	0.17, 0.21, 0.31, 0.40, 0.49, 0.57, 0.64

The PEPT system included radioactively labelled tracers, a positron camera, and an algorithm. The tracer particles were randomly selected from the bulk materials and radioactively labelled using ^{18}F, which decayed by β^+ decay with the emission of positrons (Fan et al., 2006a, 2006b). Each positron rapidly annihilated with an electron, emitting a pair of counter-propagating 511 keV γ-rays. The positron camera consisted of two γ-ray detectors, which were placed vertically by each side of the fluidized bed column. Each detector covered a field of approximately 590 × 470 mm^2. A location algorithm calculated a point which minimises the sum of perpendicular distances to the various lines of response, and discarded the events with lines of response that lie far from the point. The point that minimised the sum of perpendicular distances was then recalculated using the remaining lines of response. This process continued by iteration until all corrupt events were discarded. In favourable conditions, the algorithm determined the tracer location to within 1 mm approximately once per millisecond. The particle position as the function of time, instantaneous particle velocity at a position, probability of the tracer particle to be located at a specific position within the equipment domain, time-averaged tracer particle velocity vector map, particle occupancy map, and particle kinetic energy map can be obtained through the PEPT technique.

All experiments were carried out in the bubbling regime. The packed bed height was 1, 1.5 and 2 times of the bed diam-